Eur. Phys. J. D **38**, 111–115 (2006)
DOI: 10.1140/epjd/e2006-00041-3

THE EUROPEAN PHYSICAL JOURNAL D

The azimuthal dependent oxidation process on Cu(110) by energetic oxygen molecules

K. Moritani[1,a], M. Okada[2], T. Fukuyama[2], Y. Teraoka[1], A. Yoshigoe[1], and T. Kasai[2]

[1] Synchrotron Radiation Research Center, Japan Atomic Energy Research Institute, 1-1-1 Kouto, Mikazuki, Sayo, Hyogo 679-5148, Japan
[2] Department of Chemistry, Graduate School of Science, Osaka University, 1-1 Machikaneyama-cho, Toyonaka, Osaka 560-0043, Japan

Received 16 August 2005
Published online 21 February 2006 –

Abstract. We report a study on the oxidation process induced by a hyperthermal oxygen molecular beam (HOMB) on Cu(110) using X-ray photoemission spectroscopy in conjunction with a synchrotron radiation source. The oxidation process induced by energetic O_2 beams on Cu(110), depending on the azimuthal angle of incidence, suggests that the –Cu–O– added row structure has a role in inhibiting adsorption as a steric obstacle for incident O_2 molecules.

PACS. 68.43.Fg Adsorbate structure (binding sites, geometry) – 68.43.Jk Diffusion of adsorbates, kinetics of coarsening and aggregation – 68.47.De Metallic surfaces – 68.49.Uv X-ray standing waves

1 Introduction

Cu_2O is an industrially important semiconductor, especially for application in solar cells [1]. Both higher carrier density and lower leakage currents are required for improved performance in terms of energy conversion in Cu_2O-based solar-cell devices. Thus, it is necessary to improve the quality of Cu_2O films, although an amorphous phase is frequently used [2]. Oxidation using hyperthermal O_2 molecular beams (HOMB) with incident energies of 1∼10 eV is one of the best candidates for an efficient and controllable method for Cu_2O film formation. At higher incident energies (above 10 eV), sputtering effects [3] make it difficult to control the processes and the quality of the resultant films. Recently, we reported studies on the formation of Cu_2O induced by HOMB on Cu(100) and Cu(111) [4,5] surfaces and proposed a collision-induced absorption (CIA) mechanism. Since the oxidation process depends strongly on the crystal plane of the copper [6,7], it is important to investigate a face-dependent oxidation process based on HOMB for fabricating good quality thin films of Cu_2O in a efficient and tunable way.

The oxygen incorporation process on an open surface such as (110) seems to be more complicated on the contrary to the (100) and (111) case. Since there are many kinds of directly accessible sites on (110) surface where the atoms beneath the surface layer are revealed and the surface is highly corrugated because of the atomic row along the two azimuthal direction of [001] and [1$\bar{1}$0]. On the highly corrugated surface sticking probability cannot scale with normal energy $E_i\cos^2\theta_i$(E_i: incident kinetic energy, θ_i: angle of incidence with respect to the surface normal), because the parallel momentum connected to the surface corrugation plays an important role in contrast to the flat surface [8]. Some researchers investigated the initial sticking probability (S_0) on (110) surface by using molecular beam techniques. Vattuone et al. reported the anisotropy of the S_0 of O_2 depending on the azimuthal angle of incidence on Ag(110) and concluded that the strong anisotropy of the potential of the molecular precursor state affects the azimuthal anisotropy of S_0 [9], while Hodgeson et al. reported a substantial insensitivity of the S_0 of O_2 on Cu(110) where no molecular precursor was present [10]. In spite of these detailed experimental studies about the dissociative adsorption on (110) surface, the azimuthal dependence of sticking probability (S) during the oxidation process has not been investigated.

Here we present the unique reaction dynamics on Cu(110) surface induced by HOMB during the oxygen adsorption processes including the Cu_2O formation. The oxygen sticking probability on Cu(110) is larger than that on (100) and (111) by 2∼3 orders of magnitude at the same atomic density of oxygen adatoms. And also we found that the sticking probability during oxygen-molecule incidence along the [1$\bar{1}$0] direction is smaller than that against the [110] direction on Cu(110) surface. These results suggest that the active sites shaded by the $p(2\times1)$-O added row structure play a key role at the higher reactivity on Cu(110) surface.

[a] e-mail: moritani@spring8.or.jp

In this paper we report a study of the HOMB-induced oxidation process on open Cu(110) surfaces using X-ray photoemission spectroscopy (XPS) in conjunction with a synchrotron radiation (SR) source, and we demonstrate the unique possibility of the Cu_2O formation on the (110) face by HOMB even at room temperature.

2 Experimental

All experiments were performed with the surface reaction analysis apparatus (SUREAC 2000) constructed at BL23SU in SPring-8 [11]. The base pressure of surface reaction chamber was about 2×10^{-8} Pa. The Cu(110) sample was cleaned by repetition of 1-keV-Ar^+ sputtering and annealing at 870 K until no impurity was detected by XPS with SR and low-energy electron diffraction (LEED) showed a sharp 1×1 pattern with low background. The O_2 molecules are dosed on the Cu(110) by the backfilling of the O_2 gas at $1.33\times10^{-5}\sim1.33\times10^{-4}$ Pa or HOMB seeded in He. The incident energy of the HOMB was calculated to be 2.3 eV at nozzle temperature of 1400 K. The incident direction of the HOMB is along the surface normal of the sample or along oblique direction tilted 45° from the surface normal direction with azimuthal angle of direction along the high symmetry directions $[1\bar{1}0]$ and [100]. The flux density of O_2 molecules when the HOMB was irradiated at the sample position was experimentally estimated. The estimation method is described elsewhere [12]. The estimated flux density of O_2 molecules at the sample position was $\sim2\times10^{14}$ molecules $cm^{-2}\,s^{-1}$ in the normal incidence case. The back ground pressure and oxygen partial pressure during the HOMB irradiation were 5×10^{-6} Pa and 1×10^{-7} Pa, respectively. After irradiation of a proper amount of HOMB, high-resolution XPS spectra were measured by a hemispherical electron energy analyzer which direction was surface normal, using a monochromatic SR beam. We also observed the LEED pattern of the Cu(110) surface after measurements of XPS spectra. All experiments were performed at the sample temperature of 300 K.

3 Results and discussions

Figure 1 shows the typical evolution of the O-1s SR-XPS spectra during 2.3-eV-HOMB irradiation along the surface normal on a Cu(110) surface at 300 K. The O coverage (Θ) was determined from the O-1s intensity in comparison with Cu(100)-$(2\sqrt{2}\times\sqrt{2})R45°$–O ($\Theta = 0.5$ ML) with a correction for the face-dependent Cu density. A symmetric single O-1s peak appeared at 529.9 eV and intensified at the same position with increasing Θ up to 0.64 ML. At higher Θ, the peak can be separated into two components; one at 529.9 eV and the other at a higher binding energy corresponding to the surface and subsurface (Cu_2O) O atoms, respectively [13]. A (2×1) LEED pattern corresponding to $p(2\times1)$-O-added row (AR) [14] began to appear above 0.1 ML. After the (2×1) structure was fully developed at ∼0.5 ML, the $c(6\times2)$ LEED pattern [15] started to appear and was completed at ∼0.7 ML. In all cases, all the oxygen adsorbed dissociatively, because no peak is located above 532 eV.

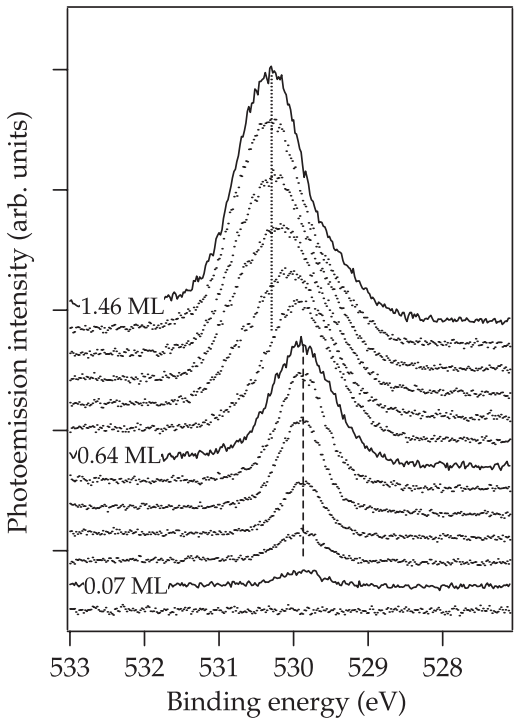

Fig. 1. Dependence on O-coverage of O-1s SR-XPS peak on Cu(110) for the 2.3-eV-HOMB incidence normal to the surface at 300 K.

Figure 2 shows the incident-energy dependent O-uptake curves determined from the area of the corresponding O-1s XPS peaks. The larger initial sticking efficiency for thermal O_2 than that for the 2.3-eV HOMB suggests the presence of precursor-mediated adsorption at low incident energy. The decrease in initial sticking efficiency for 2.3-eV-HOMB irradiation is explained by the shorter residence time of the nonadiabatic trapping state of O_2^- and/or O_2^{2-} in the direct scattering process at a higher E_i since the wave packet evolution into the dissociation channel depends on the residence time of the trapped wave function. The coverage of Θ for the thermal O_2 exposure almost saturated at ∼0.5 ML. For the thermal O_2, a huge dosage of $\sim10^5$ L, corresponding to $\sim10^{19}$ molecules cm^{-2}, was required to produce the $c(6\times2)$ structure at 300 K [6,15–17] and it was rather difficult to promote oxidation beyond 0.7 ML [18] because of the strong repulsive interaction between the O adatoms [19]. In contrast, 2.3-eV HOMB easily achieved Θ over 0.5 ML and the resulting formation of Cu_2O was more *efficient*. These facts would imply that hyperthermal O_2 could easily overcome the activation barrier of dissociative adsorption in this coverage region. The $c(6\times2)$ structure was maintained even at $\Theta \geq 0.7$ ML for 2.3-eV HOMB.

Figure 3 shows the dependence of the S on O-atom density during 2.3-eV-HOMB oxidation on Cu surfaces, as determined by differentiation of the corresponding

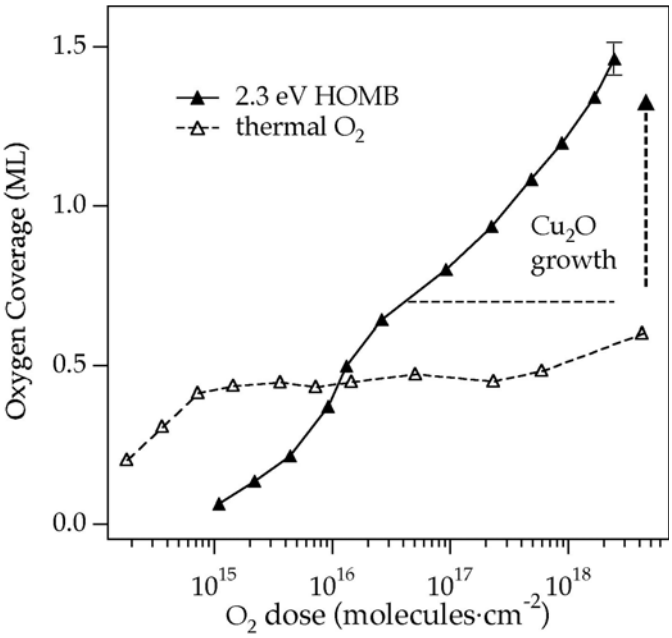

Fig. 2. O-uptake curves for 2.3-eV (triangles with solid lines) and thermal O_2 dose (open triangles with broken lines) on Cu(110). The dashed line indicates the surface O contribution. The ML unit represents the number of atoms per surface Cu atom. The uptakes determined by integration of the O-1*s* SR-XPS spectra.

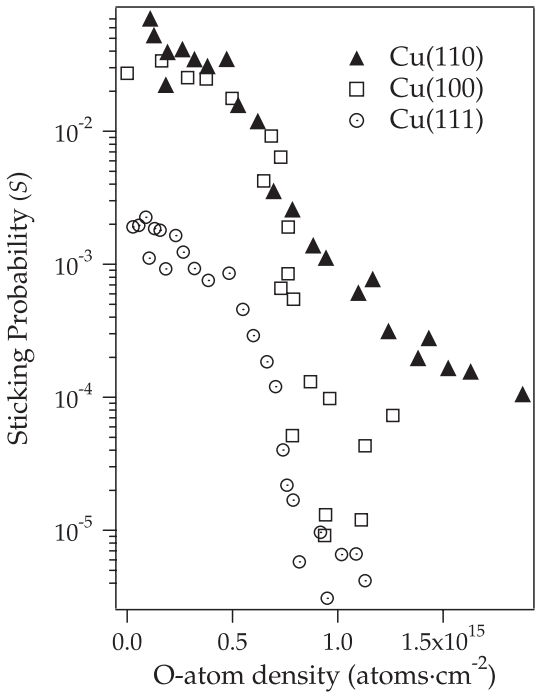

Fig. 3. O-atom-density dependence of the sticking probability during the 2.3-eV-HOMB oxidation of Cu(110) (solid triangles), Cu(100) (open squares) and Cu(111) (open circles). HOMB was irradiated along the surface normal at 300 K.

uptake curves. The value of S on (100) and (111) surfaces decreases suddenly around 8×10^{14} atoms cm^{-2} ($\Theta \sim 0.5$ ML) and then maintains a low probability of 10^{-5}∼10^{-6} during Cu_2O formation, so the attainable O density in the possible exposure range is lower than that on (110). The relatively low value of S has been interpreted by the CIA process [4,5]. On the other hand, the value of S during the formation of Cu_2O on Cu(110) is larger by 1∼2 orders of magnitude than those obtained on (100) and (111) surfaces. In order to verify the possibility of the collision-induced-absorption mechanism, we measured the O-1*s* spectra after the 3-eV-Ar-beam incidence along the surface normal on the Cu(110) surface that was saturated by the thermal O_2 gas adsorption at ∼300 K. Even after the 3-eV-Ar dose of 6.5×10^{20} atoms cm^{-2}, no noticeable changes in the line shape of the O-1*s* peak were observed. It is considered that no efficient incorporation of O atoms were induced on Cu(110) by the energetic Ar beam. It should be noticed that the Cu_2 O formation was clearly induced by $\sim 10^{19}$ atoms/cm^2 of 3-eV Ar on Cu(100) [4]. Thus, the larger value of S on (110) cannot be explained entirely by the CIA mechanism with a low cross-section. The formation of the defects and/or disordered local structure during the HOMB irradiation can be disregarded, since the $p(2 \times 1)$ LEED pattern was observed after 3-eV-Ar-beam irradiation. Thus, we have to consider other efficient mechanism of oxidation which is peculiar to Cu(110) surface.

In Figure 4, we show the azimuthal-angle dependence of the uptake curve for the 2.3-eV-HOMB incidence. The angle of incidence is 45° from the surface normal along the [001] direction (along AR) or along the [1$\bar{1}$0] direction (normal to AR). At the low oxygen coverage below 0.2 ML, the sticking efficiency is insensitive to the incident azimuth. With increasing oxygen coverage above 0.2 ML, dissociative adsorption along AR occurs more efficiently than normal to AR; i.e., the value of S along AR is larger than that along normal to AR. The clean Cu(110) surface seen by the O_2 molecules is flatter than the $p(2\times1)$-O surface, since the initial sticking probability of S_0 is independent of the incident azimuth on the clean surface [10]. The onset of the difference in efficiency occurs at $\Theta \sim 0.2$ ML, almost corresponding to the appearance of AR, although the S is initially independent of the incident azimuth. Figure 4 clearly shows that the azimuthal anisotropy of the oxidation efficiency is connected to this highly corrugated AR structure. It should be noted in Figure 4 that the oxidation efficiency along AR is nearly the same as that for the normal incidence for $\Theta \leq 0.7$ ML.

We propose the following reaction mechanism based on the experimental results. The HOMB oxidation on Cu(110) proceeds via dissociation at troughs of the AR structure for $\Theta \leq 0.7$ ML, possibly via precursors. According to theoretical studies, a 4-fold hollow site on a Cu(110) surface is favorable for O_2 adsorption followed by spontaneous dissociation [20]. Such a hollow site on the AR structure is accessible by HOMB along both AR

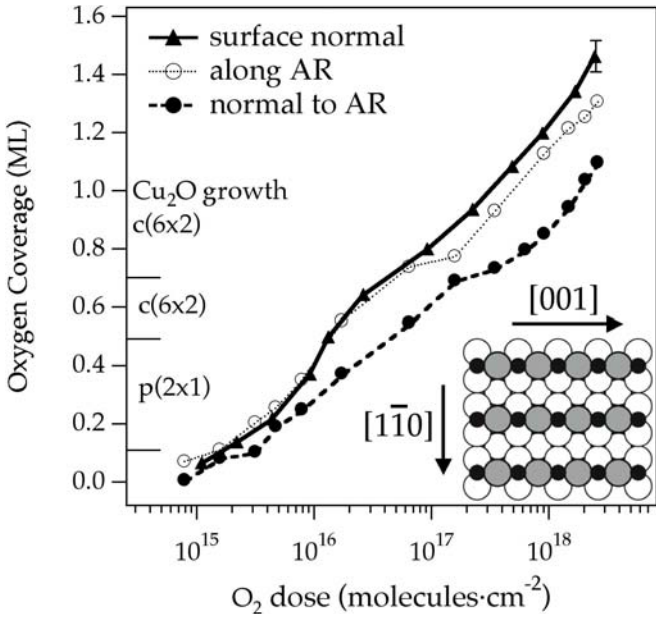

Fig. 4. The azimuthal-incident-angle dependence of the uptake curves on Cu(110) at 300 K with a schematic drawing of the AR structure. The solid triangles and line, the open circles and thin dotted line and the solid circles and broken line are the O-uptake curves for the 2.3-eV-HOMB irradiation along the surface normal, along the [001] direction (along AR) and along the [1$\bar{1}$0] direction (normal to AR), respectively. The angle of the oblique incidence is 45° from the surface normal. The observed LEED patterns are indicated at the left. The inset shows a schematic drawing of the surface structure of $p(2 \times 1)$-O added row structure of Cu(110) and the corresponding azimuthal direction. The large gray circles, the small black circles and the white large circles are surface Cu atoms, O atoms and Cu atoms below the surface layer, respectively.

and the surface normal without any shadowing effect. On the other hand, the corrugation by the AR structure is so large that it inhibits the dissociation of the O_2 molecules impinging along the normal to AR by the shadowing effect, although Darling et al. demonstrated that the parallel momentum mainly enhanced the dissociation on the geometrically corrugated surface [8]. This scenario is also applicable to the oxidation process for $\Theta \geq 0.7$ ML. On the $c(6\times2)$ structure, copper atoms occupy alternate short bridge sites along the [001] rows in the trough and shadow reactive sites in the trough from the HOMB, even along AR [21]. This may cause a reduction in S for the HOMB incidence along AR for $\Theta \geq 0.7$ ML compared to the normal incidence (see the solid triangles and the open circles for $\Theta \geq 0.7$ ML in Fig. 4).

The energy barrier for access to the reactive site on the $c(6 \times 2)$ structure is enhanced due to the repulsive interaction between the existing –Cu–O– chains and an impinging O_2 molecule, and thus a high translational energy is required for further oxidation when $\Theta \geq 0.7$ ML. In addition to dissociation at the hollow site, the reaction possibly occurs via newly-formed active sites. The 2.3-eV HOMB has large translational energy compared with the diffusion barrier of the surface adatoms, which is generally several hundred meV [19]. Thus, the 2.3-eV HOMB may promote the diffusion of copper atoms by local heating in the energy dissipation of HOMB. In this case, a migrating Cu atom (possibly in the trough) works as a reactive site. The face-dependent oxidation process may come from the openness of the (110) surface compared with (111) and (100) surfaces. The lower diffusion barrier for Cu and O atoms on (110) [19] compared to the other faces [22] makes it easier to produce dissociation sites that are accessible only by higher energy HOMB for $\Theta \geq 0.7$ ML. According to theoretical calculations, the adsorption of O-atoms reduces the diffusion barrier of the Cu atom [22], which may be of further help in creating new dissociation sites. Once surmounting the activation barrier and adsorbing on the surface, oxygen atoms can easily move to the subsurface sites and form Cu_2O above 0.7 ML at 300 K [13].

4 Summary

In summary, oxidation of Cu(110) by energetic O_2 beam was investigated by XPS in conjunction with SR. The 2.3-eV HOMB promotes the oxidation more effectively than the thermal O_2 gas above 0.5 ML. The sticking probability on Cu(110) is larger by 1∼2 orders of magnitude than those obtained on (100) and (111) surfaces during the Cu_2O incorporation by 2.3-eV HOMB, although the effect of CIA process is so small on Cu(110). There is large anisotropy of sticking probability depending on the azimuthal direction of incident which is connected the $p(2 \times 1)$ added row reconstructed structure. The newly opened reaction channel via the troughs of the AR structure by the 2.3-eV HOMB and shadowing effect from the reactive hollow site can explain the oxidation mechanism on the Cu(110) surface.

All of the experiments were performed using SUREAC2000 at BL23SU in SPring-8. The authors are thankful to Y. Saitoh and S. Fujimori for their help with the operation of the monochromatic system at the beam line. The group at Osaka University is financially supported by the 21st Century COE program and CREST of JST. MO gratefully acknowledges the Hyogo Science and Technology Association, and also the Japanese Ministry of Education, Culture, Sports, Science and Technology for a Grant-in-Aid for Scientific Research (No. 17550011).

References

1. L.C. Olsen, F.W. Addis, W. Miller, Solar Cells **7**, 247 (1982/1983)
2. Y. Okamoto, S. Ishizuka, S. Kato, T. Sakurai, N. Fujiwara, H. Kobayashi, K. Akimoto, Appl. Phys. Lett. **82**, 1060 (2003)
3. M. Okada, Y. Murata, Surf. Sci. **291**, 451 (1993)
4. M. Okada, K. Moritani, S. Goto, T. Kasai, A. Yoshigoe, Y. Teraoka, J. Chem. Phys. **119**, 6994 (2003)

5. K. Moritani, M. Okada, S. Goto, S. Sato, T. Kasai, A. Yoshigoe, Y. Teraoka, J. Vac. Sci. Technol. A **22**, 1625 (2004)
6. F. Jensen, F. Besenbacher, E. Lægsgaard, I. Stensgaard, Phys. Rev. B **41**, 10233 (1990)
7. F. Jensen, F. Besenbacher, E. Lægsgaard, I. Stensgaard, Phys. Rev. B **42**, 9206 (1990)
8. G.R. Darling, S. Holloway, Surf. Sci. Lett. **304**, L461, (1994)
9. L. Vattuone, C. Boragno, M. Pupo, P. Restelli, M. Rocca, U. Valbusa, Phys. Rev. Lett. **72**, 510 (1994)
10. A. Hodgson, A.K. Lewin, A. Nesbitt, Surf. Sci. **293**, 211 (1993)
11. Y. Teraoka, A. Yoshigoe, Jpn J. Appl. Phys. **38** (Suppl. 1), 642 (1999)
12. Y. Teraoka, A. Yoshigoe, Jpn J. Appl. Phys. **41**, 4253 (2002)
13. A.P. Baddorf, J.F. Wendelken, Surf. Sci. **256**, 264 (1991)
14. D.J. Coulmann, J. Wintterlin, R.J. Behm, G. Ertl, Phys. Rev. Lett. **64**, 1761 (1990)
15. R. Feidenhans'I, F. Greym, M. Nielsen, F. Besenbacher, F. Jensen, E. Lægsgaard, I Stensgaard, K.W. Jacobsen, J.K. Nørskov, R.L. Johnson, Phys. Rev. Lett. **65**, 2027 (1990)
16. J.M. Mundener, A.P. Baddorf, E.W. Plummer, L.G. Sneddon, R.A. Didio, D.M. Zehner, Surf. Sci. **188**, 15 (1987)
17. D. Coulmann, J. Wintterlin, J.V. Barth, G. Ertl, R.J. Behm, Surf. Sci. **240**, 151 (1990)
18. G.R. Gruzalski, D.M. Zehner, J.F. Wendelke, R.S. Hathcock, Surf. Sci. **151**, 430 (1985)
19. S.Y. Liem, G. Kresse, J.H.R. Clark, Surf. Sci. **415**, 194 (1998)
20. S.Y. Liem, J.H.R. Clark, G. Kresse, Surf. Sci. **459**, 104 (2000)
21. G. Dorenbos, N. Breeman, D.O. Boerma, Phys. Rev. B **47**, 1580 (1993)
22. M. Alatalo, S. Jaatinen, P. Salo, K. Laason, Phys. Rev. B **70**, 245417 (2004)